Multistatic Gen2 RFID over Ethernet with Commodity SDRs

Michail Ouroutzoglou†, Georgios Vougioukas†, Panos N. Alevizos†, Antonis G. Dimitriou* and Aggelos Bletsas†
†School of ECE, Technical University of Crete, Chania 73100, Greece
* Dept. of ECE, Aristotle University of Thessaloniki, Thessaloniki 54453, Greece

***Abstract*—Industrial Gen2 RFID tags are limited by the tag's RF energy harvesting sensitivity, requiring relatively strong signals that impinge on the tag's antenna. Prior art has proposed dense reader antenna networks, that effectively bring the illuminating antenna closer to the tag, using either networks of RF cables, multiplexers and RF amplifiers or custom RF front-ends, wired to a baseband processor or even custom wireless RF front ends with proprietary protocols. This work distributes Gen2 operation and proposes multistatic networks of commodity, low-cost, software defined radios (SDR), connected over the (nowadays omnipresent) Ethernet. Thus, this work puts forth distributed reception of Gen2 RFID with potentially reduced (installation) cost. Bit error rate (BER)-optimal coherent and near-optimal noncoherent, linear complexity Miller sequence detection are tested, adhering to real time processing constraints. Experimental results demonstrate that under real time carrier frequency offset estimation with phased-lock loop (PLL), Gen2 RFID tags can be detected reliably, without rate-limiting preamble pilot bits, while more than one distributed SDR transmitters can boost area coverage. Multistatic setups allow for higher probability the tag antenna will be found closer to sufficiently strong illuminating field, overcoming the limitations of existing RF energy harvesting technology. Hopefully, this work will spark interest towards the convergence of Gen2 RFID with (current) Ethernet or (future) cellular telephony industry.**

I. Introduction

Existing batteryless radio frequency identification (RFID) tags currently balance between two conflicting tasks: absorb radio frequency (RF) energy as much as possible for self-powering, while reflecting RF, i.e., backscattering as much as possible for communication of their information. However, the limiting factor is the tag's RF energy harvesting circuitry sensitivity [1], requiring relatively strong signals that impinge on the tag's antenna.

It was recently shown that bistatic [2]–[5] or multistatic [6]–[9] backscatter radio architectures can increase range and coverage; in such architectures, one (or several) RF illuminator(s) are utilized far apart from the receiver of the backscattered signals, taking full advantage of the dyadic [10], nonlinear character of wireless propagation and offering both link budget and diversity advantage, compared to conventional *monostatic* architectures; in the latter, transmit and receive antennas belong to the same reader unit. However, non-monostatic architectures increase complexity and cost of installation. Bistatic architectures have been also proposed in the literature, where the tags backscatter signals, compatible with Bluetooth [11], [12], WiFi [13] or Lora [14] reception. However, all the aforementioned papers in this paragraph did not focus on multistatic architectures for the industrial (Gen2) RFID protocol.

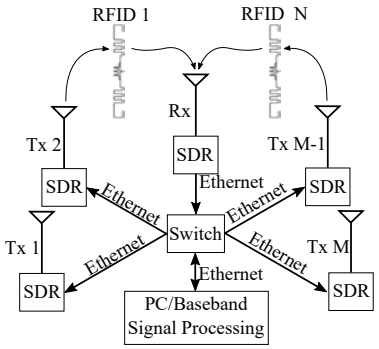

Fig. 1: Architecture of the proposed real-time, Ethernet-based network of low-cost SDRs interrogating Gen2 RFID tags.

The RFID industry/research community has proposed several ways to bring the illuminating antenna closer to the tag, increasing the number of transmitting antennas in a given area; one way is by using wired networks of multiplexers, RF cables and amplifiers, so that several distributed antennas illuminate a population of tags [15]; another way is to build a custom star-topology wireless network of distributed illuminators and a single receiver, exchanging messages with a proprietary protocol [15]; alternatively, monostatic, custom front ends are distributed and wired to a baseband processor [16]. Installations of RFID readers on robotic, mobile platforms have also appeared in commercial applications (e.g., robotic assistants), as well as designs for mobile relays [17].

This work studies a multistatic setup, where commodity, low-cost, software-defined radios (SDR) - instead of custom RF frontends - act as transmit/receive frontends, acquiring/delivering baseband signal samples, through standard Ethernet local area network (LAN) infrastructure. The latter is currently omnipresent in building infrastructure, minimizing installation and overall cost:

- Through Ethernet, the baseband samples are transferred to/from a commodity personal computer (PC), where they are processed/generated (Fig. 1).
- Gen2 industrial RFIDs are tested and real-time processing challenges, relevant to carrier frequency offset (CFO), are studied and addressed.
- Real-time processing challenges relevant to low-complexity, BER-optimal coherent and near-optimal non-

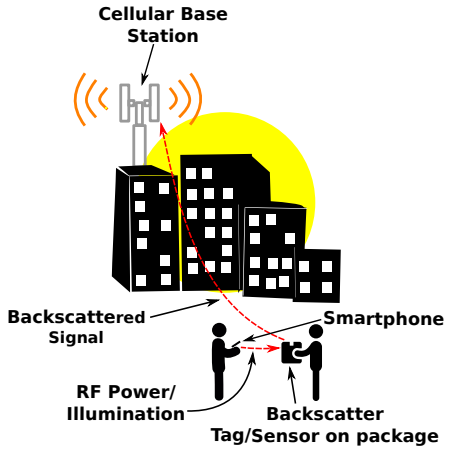

Fig. 2: Convergence Vision: Could existing (e.g., LAN) or future (e.g., cellular) network infrastructure read commercial (Gen2) RFID tags?

coherent Miller sequence detection, are overcome. Due to distributed operation and remaining CFO, careful noncoherent detection of Miller sequences becomes critical.

- It is shown that commodity, low-cost SDRs, connected over the Ethernet, in conjunction with the proposed intelligent, real-time signal processing, can successfully read Gen2 tags, with the advantages of multistatic architecture, while reducing installation costs, due to Ethernet.
- Limitations of the proposed techniques are also discussed.

Our inspiration is shown in Fig. 2. Could a cell phone illuminate a Gen2 RFID-tagged package, with tag-backscattered information received by the pico/femto-cell? In that way, existing RFID technology, apparatus and know-how could be exploited in future telecommunications infrastructure. Stringent timing requirements in Gen2 challenge such vision. This work shows how Ethernet/LAN infrastructure can be used for Gen2 RFID reception. Hopefully future work will contribute towards the cellular telephone-RFID convergence vision.

Section II offers the system model; Section III offers the system architecture, emphasizing on the overall signal processing steps, as well as details on housekeeping tasks (e.g., CFO correction); Section IV offers a summary of the Miller sequence detection techniques of linear complexity; Section V offers experimental results; Section VI discusses limitations of proposed system and finally, work is concluded in Section VII.

Notation: $\mathcal{CN}(\mathbf{m}, \mathbf{C})$ denotes the proper complex Gaussian distribution of mean $\mathbf{m}$ and covariance matrix $\mathbf{C}$. The conjugate of a complex number w is denoted as w^H; in the case of a complex vector $\mathbf{z}$, conjugate transpose (hermitian) is denoted also as $\mathbf{z}^H$. The inner product of two complex vectors $\mathbf{u}, \mathbf{v}$ is denoted as $\langle \mathbf{u}, \mathbf{v} \rangle = \mathbf{u}^H \mathbf{v}$. The real part of a complex number w is given by $\Re\{w\}$.

II. System Model

A network of $M+1$ distributed (in space) SDRs is considered (Fig. 1), connected over 1 GBit Ethernet LAN. A single SDR is serving as the receiver, while M transmitting SDRs, operating in a switched manner, provide the appropriate illumination and query signals; there is no need for simultaneous transmissions from different transmitting SDRs. Baseband samples are communicated over the Ethernet between the SDRs and a (commodity) laptop computer, with the latter performing the necessary signal processing tasks.

The general system model for the SDR samples assumes the following form [5]:

$$\begin{aligned} \mathrm{y}[k] &= \left(\sqrt{2P_\mathrm{c}}h_\mathrm{CR} + \sqrt{2P_\mathrm{c}}h\,\mathrm{s}\,\mathrm{x}_\mathrm{tag}\left[k\right]\right)\mathrm{e}^{-\mathrm{j}(2\pi\Delta f k T_\mathrm{s}+\Delta\phi_\mathrm{R})} \\ &\quad + \mathrm{n}[k] \\ &= \left(m_\mathrm{dc} + m_\mathrm{tag}\mathrm{x}_\mathrm{tag}\left[k\right]\right)\mathrm{e}^{-\mathrm{j}(2\pi\Delta f k T_\mathrm{s}+\Delta\phi_\mathrm{R})} + \mathrm{n}[k]\,, \quad (1) \end{aligned}$$

where T_s, Δf, $\Delta\phi_\mathrm{R}$ is receiver's sampling period, carrier frequency and phase offset (CFO, CPO), respectively; Tag's signal $\mathrm{x}_\mathrm{tag}\left[k\right] \in \{\Gamma_0, \Gamma_1\}$, where Γ_0, Γ_1 correspond to the reflection coefficients for bit "0" and "1", respectively; P_c is the transmission power of the illuminating carrier's signal and $\mathrm{s} \in (0,1)$ denotes the tag's scattering efficiency; receiver thermal noise is modeled by $\mathrm{n}[k] \sim \mathcal{CN}\left(0, \sigma_\mathrm{n}^2\right)$, where $\sigma_\mathrm{n}^2 = N_0 W_\mathrm{rx}$, N_0 stands for the noise power spectral density and W_rx denotes receiver's bandwidth; different noise samples (i.e., $\mathrm{n}[k], \mathrm{n}[m], k \neq m$) are independent. Flat fading is assumed and effects of multipath are modeled by $h_\mathrm{CR} \in \mathbb{C}$ and $h = h_\mathrm{CT}h_\mathrm{TR} \in \mathbb{C}$:

$$h_\mathrm{q} \sim \mathcal{CN}\left(\sqrt{\frac{\mathrm{k_q}}{\mathrm{k_q}+1}\sigma_\mathrm{q}^2}, \frac{\sigma_\mathrm{q}^2}{\mathrm{k_q}+1}\right),\ q \in \{\mathrm{CR}, \mathrm{CT}, \mathrm{TR}\}\,, \quad (2)$$

where $\mathrm{CR}, \mathrm{CT}, \mathrm{TR}$ denote the carrier/illuminator-to-receiver, carrier-to-tag and tag-to-receiver links, respectively, and $\sigma_\mathrm{q}^2 = \mathbb{E}\left[|h_\mathrm{q}|^2\right]$. Parameter $\mathrm{k_q}$ is the power ratio of the dominant (line-of-sight) path over the scattered paths (Rician fading). For $\mathrm{k_q} = 0$, Rayleigh fading is obtained. Complex gains h_q are assumed constant for the duration of a backscattered packet and change independently between successive packets.

It is noted that tag's structural mode parameter $A_\mathrm{s} \in \mathbb{C}$ is absorbed in the dc term m_dc.

III. Architecture

A. Distributing The Gen2 Protocol Operation

In Gen2 RFID, the interrogating device (reader) initiates the communication, by transmitting a QUERY-command signal. Using the latter, the reader is able to configure various communication-related parameters (e.g., tag's rate, line encoding). Multiple access is performed according to the slotted Aloha protocol, while the number of slots is configured by the QUERY command. After receiving the QUERY signal, the tag backscatters a random 16-bit sequence (RN16). Upon detection of that sequence, the reader re-transmits it back to the tag as an acknowledgement (ACK). If the ACK matches the tag's original RN16, the tag backscatters its 128-bit data sequence, which includes the electronic product code (EPC) identification information (96 bits). It has to be noted that a known preamble sequence is appended in any (backscattered)

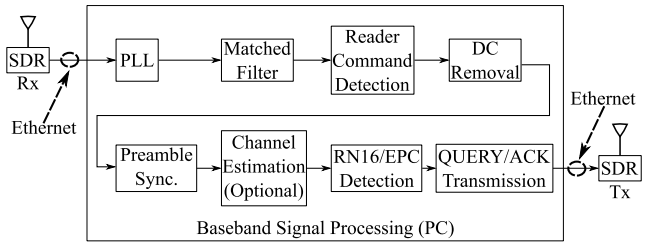

Fig. 3: Block diagram of the baseband signal processing path in the proposed system.

sequence, which can be used for synchronization and channel estimation purposes [18, 6.3.1].

Thus, transmitting (Tx) SDR (of the QUERY-command and the ACK message) is different than the receiving (Rx) SDR of the tag-backscattered RN16 and EPC information. The challenge for such distributed operation with connected SDRs over the Ethernet is further explained below.

B. Software Implementation with SDRs over Ethernet

Fig. 3 demonstrates the signal processing chain. Baseband samples are created (for transmission) and processed (for detection) in the host PC, using custom software written in C++ within the GNURadio framework, based on [19], [20]. Interrogation begins by creating the baseband samples corresponding to the QUERY command. In the absence of a reader command (QUERY, ACK), a continuous wave (CW) component is transmitted so that the tag can harvest energy for its operation. Those samples are then forwarded via Ethernet to one of the M transmitting SDRs. The receiving SDR forwards baseband I/Q samples (through Ethernet) to the host PC.

Employing separate units for transmission and reception of signals, inherently results to carrier frequency offset (CFO) between those units, due to different oscillators. To compensate for the aforementioned offset, a phase locked loop (PLL) is utilized at the receiving side. Matched filtering is then performed on the CFO-compensated samples and the QUERY command is obtained (at the receiver). Between the QUERY command and the RN16 response, there is the CW signal of the transmitter, which is used (at the receiver) to estimate the DC component, via a sample mean operation. After DC correction, synchronization with the RN16 sequence is performed, using the existing preamble bits of the Gen2 protocol. The RN16 bits can be detected either with coherent or noncoherent sequence detection, with the former requiring channel estimation. ACK command can be then constructed based on the detected RN16 sequence and be broadcast through the transmitting SDR. The reception procedure is repeated for detection of the EPC bits.

C. Real Time CFO Estimation/Housekeeping Tasks

One of the most challenging problems that needs to be solved in order to implement Ethernet/network-based multi-static RFID readers is the CFO compensation. Gen2 protocol imposes tight timing constraints, which must be satisfied for successful tag interrogation. Specifically, the time interval between backscattering (tag side) the last RN16 bit and the transmission (reader side) of the first falling edge of the ACK command *must be* under 1ms. Thus, all the involved signal processing (see Sec. III-B) and housekeeping (CFO, DC offset correction, synchronization) tasks, have to be performed relatively fast, with delay below 1ms. That is why periodogram-based, high-resolution frequency estimation, using fast fourier transform (FFT) on large blocks of received samples was not an option, especially when the goal was to simplify the utilized hardware, as much as possible. Instead, a digital phased-lock loop (PLL) is utilized, due to its real-time, control theory character.

For simulations and testing [21], a PLL was developed based on the design in [22, App. C]. A second order loop filter was utilized, with parameters fine tuned based on experimental observation of the CFO between the transmitting and receiving SDRs. Note that, in simulations, the CFO tracking occurs only during the time interval where only the CW (between QUERY and RN16/EPC) is present "in the air". That is because the developed PLL was not optimized to track CFO when information signal was present on the carrier. The rest of the samples are compensated using the solution of a least squares-based [23], best linear fit problem, utilizing the stored phases of the PLL output.

The custom PLL developed for simulations was also implemented in C++ for the real system. Even though the results were acceptable, the *PLL carrier tracking* GNURadio block was used instead. This block is connected between the source (receiving SDR) and the matched filter blocks (Fig. 3) and it's active, throughout the whole interrogation process. Details on the real-time character of optimal Miller-encoded tag-backscattered sequence detection (i.e., for either RN16 or EPC) follow.

IV. Detection

Assuming perfect CFO compensation, matched filtering, DC offset removal and synchronization, the signal model of Eq. (1) adheres to the following form [20]:

$$\mathrm{y}\left[i\right] = L\sqrt{2P_{\mathrm{c}}}h\,\mathrm{s}\,\mathrm{x}_{\mathrm{tag}}[i] + \mathrm{w}\left[i\right], \tag{3}$$

i denotes the sample index, $L = \frac{T_{\mathrm{b}}}{4T_{\mathrm{s}}}$ is the oversampling factor, $\mathrm{x}_{\mathrm{tag}}[i] \in \{0,1\}$ and $\mathrm{w}\left[i\right] \sim \mathcal{CN}\left(0, L\sigma_{\mathrm{n}}^2\right)$. Assuming Miller 2 line encoding and N backscattered bits, Eq. (3) can be rewritten in vector form, as follows [24]:

$$\mathbf{y}[n] = \begin{bmatrix} y[4n+0] \\ y[4n+1] \\ y[4n+2] \\ y[4n+3] \end{bmatrix} = \tilde{h}\mathbf{x}[n] + \mathbf{w}[n],\ n = 0, 1, \ldots, N-1, \tag{4}$$

where $\tilde{h} = L\sqrt{2P_{\mathrm{c}}}h\,\mathrm{s}$, $\mathbf{w}[n] \sim \mathcal{CN}\left(0, L\sigma_{\mathrm{n}}^2\mathbf{I}_4\right)$ and data vectors $\mathbf{x}[n] \in \mathbb{S} = \{\mathrm{S1},\ \mathrm{S2},\ \mathrm{S3},\ \mathrm{S4}\}$. Intuition behind the above equivalence is offered by the allowed Miller line

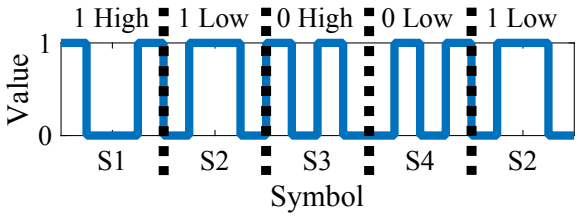

Fig. 4: Graphical representation of Miller-2 waveforms.

transitions, shown in Fig. 4, while respective vectors in $\mathbb{S}$ are given by:

$$\mathrm{S1} = \begin{bmatrix}1 & 0 & 0 & 1\end{bmatrix}^T,\ \mathrm{S2} = \begin{bmatrix}0 & 1 & 1 & 0\end{bmatrix}^T,$$
$$\mathrm{S3} = \begin{bmatrix}1 & 0 & 1 & 0\end{bmatrix}^T,\ \mathrm{S4} = \begin{bmatrix}0 & 1 & 0 & 1\end{bmatrix}^T.$$

A. Miller Line Code

Specifically, Miller 2 line encoding offers 4 possible line waveforms, two for bit-0 and two for bit-1 (Fig. 4). The waveforms for bit-0 alternate the line level at the middle of the bit, as opposed to bit-1, where the level remains constant (at the middle of the bit). Additionally, the line level at the beginning of each bit, must change compared to the line level at the beginning of the previous bit. The only exception to the previous rule is when there is a bit-0 to bit-1 transition. Fig. 4 visualizes examples of allowed transitions, while Fig. 5 depicts all possible transitions. Clearly, Miller line code induces memory on the backscattered sequence, which means that the line-encoded, consecutive tag-backscattered symbols in $\mathbb{S}$ are not independent; thus, optimal detection requires sequence and not symbol-by-symbol detection.

It is also noted that the above methodology and formulation can be easily and directly extended to Miller 4 and Miller 8 waveforms; such extension is omitted, due to space constraints and will be reported elsewhere [21].

B. Coherent Sequence Detection

Given perfect channel state information (CSI), the optimal sequence can be found by solving a maximum likelihood (ML) problem [24], [25] shown in the lemma below:

Lemma 1. *Let $\hat{\mathbf{x}}[n] \in \hat{\mathbb{S}}$, $\mathbf{y}[n]$ any β-centered signal. The following holds:*

$$\hat{\mathbf{x}}^{ML} = \underset{\hat{\mathbf{x}}\in\mathcal{X}}{\operatorname{argmax}} \sum_{n=0}^{N-1} \Re\left\{\tilde{h}^H \langle \hat{\mathbf{x}}[n], \mathbf{y}[n]\rangle\right\}, \tag{5}$$

where $\tilde{h}, \mathbf{y}[n]$ refer to Eq. (4). Moverover, $\mathcal{X} \subset \hat{\mathbb{S}}^N$ is the set of all permitted N-bit Miller 2 coded sequences, and $\hat{\mathbb{S}} = \{\hat{\mathrm{S}1},\ \hat{\mathrm{S}2},\ \hat{\mathrm{S}3},\ \hat{\mathrm{S}4}\}$, defined as follows:

$$\hat{\mathrm{S}1} = \frac{1}{2}\begin{bmatrix}+1 & -1 & -1 & +1\end{bmatrix}^T,\ \hat{\mathrm{S}2} = -\hat{\mathrm{S}1},$$
$$\hat{\mathrm{S}3} = \frac{1}{2}\begin{bmatrix}+1 & -1 & +1 & -1\end{bmatrix}^T,\ \hat{\mathrm{S}4} = -\hat{\mathrm{S}3}.$$

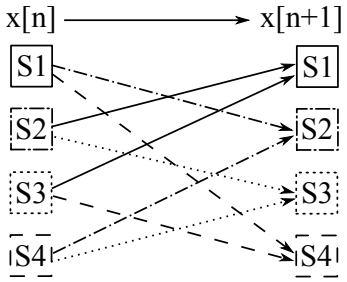

Fig. 5: Transitions allowed by Miller 2 encoding.

The maximization problem in Eq. (5) can be solved, in linear (to the sequence length) time, by the Viterbi algorithm (VA) on a trellis diagram based on Fig. 5 and weights $\mathcal{W}_{n,j} = \Re\left\{\tilde{h}^H \langle \hat{\mathbf{x}}[n], \mathbf{y}[n]\rangle\right\}$, where n denotes the nth bit and j denotes the trellis diagram state, i.e., $\hat{\mathbf{x}}[n] = \hat{\mathrm{S}}j$.

An estimate of parameter $\tilde{h}$, can be readily found using the preamble bits of Gen2, e.g., with a least squares technique. However, it is crucial to note that due to residual CFO (even after the PLL stage), this channel estimate is not robust and it deteriorates the performance of the detector in terms of bit error rate (BER) [21].

C. Noncoherent Sequence Detection

When channel coefficient $\tilde{h}$ in Eq. (4) is constant but unknown at the receiver, then, noncoherent, generalized likelihood ratio test (GLRT) sequence detection of N Miller 2 bits is equivalent to the following problem [24]:

$$\hat{\mathbf{x}}^{\mathrm{GLRT}} = \underset{\hat{\mathbf{x}}\in\mathcal{X}}{\operatorname{argmax}} \left\| \sum_{n=0}^{N-1} \langle \hat{\mathbf{x}}[n],\ \mathbf{y}[n]\rangle \right\|_2^2, \tag{6}$$

where the same notation rules apply as in Eq. (5). However, solving the above through exhaustive search among all possible N-bit sequences, entails exponential complexity of 2^N. Due to the time-critical character of the system (Sec. III-C), the linear noncoherent sequence detection algorithm proposed in [24] will be utilized.

In principle, the linear noncoherent sequence detection algorithm is a modification of the VA. Again, the trellis diagram is based on Fig. 5 and the complex weights are given by the inner product $\mathcal{W}_{n,j} = \langle \hat{\mathbf{x}}[n],\ \mathbf{y}[n]\rangle$, where n denotes the nth bit and j denotes the state of the trellis diagram, i.e., $\hat{\mathbf{x}}[n] = \hat{\mathrm{S}}j$. For every bit and state, the incoming path sum of (complex) inner products is added to that state's inner product. Then the magnitude of the complex sum is compared with that of the other 3 states, keeping the highest. The differentiation from a typical VA implementation is that, the complex weighting gains are propagated through the states, instead of the magnitude of the path that prevails.

Although this algorithm is not optimal, it has linear complexity and it has been shown to perform 0.25 dB worse than perfect CSI, ideal CFO compensation (for bistatic) or zero CFO (for monostatic) coherent sequence detection [24].

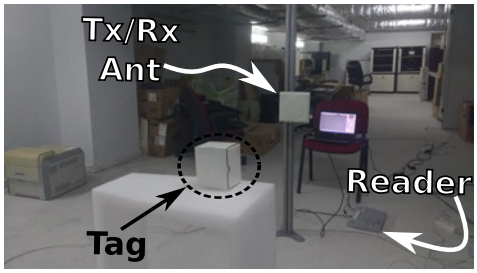

Fig. 6: Monostatic setup with commercial RFID reader under harsh indoor conditions. For transmission power of 15 dBm, a maximum communication range of 1.1 m was observed, while for 30 dBm the maximum range was 4.5 m.

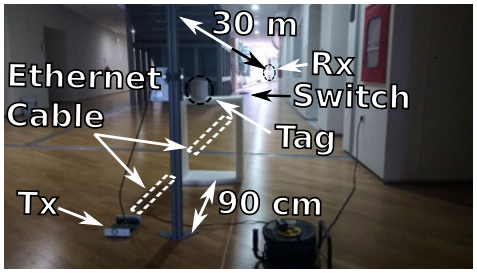

Fig. 8: Bistatic setup utilizing a single USRP as illuminating source (15 dBm) and a USRP or RTL-SDR as receiver. Carrier-to-receiver ranges of at least 30 meters were observed, for a carrier-to-tag distance of 90 cm.

V. Performance Evaluation

As baseline reference for experimental measurements under harsh indoor conditions, a monostatic setup was first tested: an Impinj Speedway R1000 RFID reader, equipped with a single antenna (Fig. 6). The reader was connected to an MTI MT-242032 7 dBi antenna via a 0.74 dB loss coaxial cable. Alien ALN-9741 (Higgs-4) and Alien ALN-9540 (Higgs-2) tags were employed. Using its application software, the reader was configured to deliver either 15 dBm or 30 dBm to the cable.[1] For the case of 15 dBm and ALN-9741 tag, the communication range was 1.1 m (away from the reader), while for 30 dBm, 4.5 m. The reader antenna was placed relatively close to the ground (0.9 m above the ground), while there were many reflective materials (Fig. 6).

The aforementioned test, set the RFID interrogation zone, outside which, the tag cannot be read; outside this zone, the tag could not operate due to the fact that the offered RF power was below its harvesting sensitivity threshold. Thus, utilizing multiple illuminating transmitters in a given space, could increase coverage.

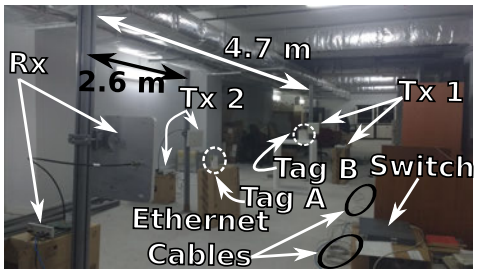

Fig. 7: Multistatic setup utilizing two USRPs as carrier sources/illuminators at 15 dBm and a RTL-SDR (or a USRP) as a receiver. The setup allows for increased coverage with distributed SDR illuminators, operating in a time-division manner and networked over Ethernet.

The setup of Fig. 7 was utilized for evaluation of the proposed, Ethernet-based, multistatic topology, in conjunction with commodity Ettus N200 USRPs and FLEX900 daughtercards. The deployment consisted of $M = 2$ transmitters (15 dBm at their output) that were connected to the aforementioned 7 dBi antennas, through a 0.45 dB loss cable. At the receiving side, a N200 was connected to an MT-242017, 10 dBi antenna. The SDRs were connected to an HP Procurve 2824 Ethernet switch, with 15 m-long, Cat5e cables. The laptop (host PC) running the baseband processing software was also connected to the switch with a Cat5e cable. In the setup of Fig. 7, $d_{\mathrm{TX1-R}} = 4.7$ m and $d_{\mathrm{TX2-R}} = 2.6$ m. Two tags were successfully interrogated. Tag A (ALN-9540) was placed at a distance of 70 cm away from Tx-2 (outside the sector defined by Tx-1), while Tag B (ALN-9741), 1.1 m away from Tx-1. The transmitters operated in a time division-switched/scheduled fashion, sequentially. If only Tx-1 was active, Tag A did not operate (and the same holds for Tx-2, Tag B). The last test, highlights the fact that the greater the number of emitters in a given area, the higher the chances of successful tag interrogation, as a wider area will offer the necessary RF power conditions, satisfying tags' RF harvesting sensitivity limitations.

Feasibility of low-cost implementation was further showcased using a 7 $ RTL-SDR dongle, tested as a receiver (connected via USB to the host PC). Using the same setup, the tag read rates corresponding to using N200 or RTL-SDR for reception, for different transmitter-to-tag distances, are offered in Table I. With increasing transmitter-to-tag distances, the tag read rate fluctuates with decreasing trend, due to indoor wireless propagation and areas where reflected signals add constructively or destructively. The limited performance of RTL-SDR is most likely caused by the large buffer size offered by its software driver, in conjunction with the low transfer speeds of USB 2.0, resulting to delays and missed blocks of samples. The system was tested using both coherent and noncoherent sequence detection schemes (see Sec. IV) and the performance, with respect to tag reading rate was similar.

The limitations imposed by the transmitter-to-tag link were further highlighted in the bistatic (single transmitter) scenario depicted in Fig. 8. In that case, the tag (ALN-9741) was placed 90 cm away from the illuminating transmitter, while the receiver was located 30 m away from the latter. The tag

[1]Cable losses as well as reader's output power were measured using a VNA and a spectrum analyzer, respectively.

	Tag Reading Rate	
Carrier-Tag Distance	N200	RTL-SDR
$d_{\mathrm{CT}} = 40$ cm	161/268	27/600
$d_{\mathrm{CT}} = 50$ cm	132/300	16/1000
$d_{\mathrm{CT}} = 60$ cm	133/600	24/1000
$d_{\mathrm{CT}} = 70$ cm	64/170	3/1000
$d_{\mathrm{CT}} = 80$ cm	124/359	18/1000
$d_{\mathrm{CT}} = 90$ cm	81/160	23/1000
$d_{\mathrm{CT}} = 1$ m	572/1000	10/1000
$d_{\mathrm{CT}} = 1.1$ cm	20/50	–

TABLE I: Tag read rates when either a USRP or an ultra-low cost RTL-SDR was used as the SDR receiver. d_{CT} denotes the carrier-to-tag distance, while the carrier-to-receiver distance was fixed to 4.7 m. The above rates are extracted out of a single run of the system. A read is considered successful when all of the EPC bits are successfully decoded.

was successfully interrogated using both N200 and RTL-SDR.

VI. Limitations

The main limitation of the Gen2 protocol is the strict time constraint between the end of the RN16 and the start of the ACK, known as $T2$. $T2$ is inversely proportional to the backscatter link frequency (BLF), i.e., the faster the tag's rate, the tighter the time constraint. In this work BLF was set to BLF $= 40KHz \rightarrow T2 = 500\mu s$. Ethernet works for small rates, however, it's an added layer that can easily become the bottleneck of the system as the tag rate increases.

VII. Conclusion

This work highlights the importance of decoupling the power delivery aspect of the RFID interrogation procedure from the communication aspect. This is possible with multi-static setups, involving multiple, low-cost SDR transmitters (and receivers), networked with Ethernet; the latter is omnipresent in existing building infrastructure, offering potential for reduced installation costs. Multistatic setups allow for higher probability the tag antenna will be found closer to sufficiently strong illuminating field, overcoming the limitations of existing RF energy harvesting technology. Hopefully, this work will spark interest towards the convergence of Gen2 RFID with (current) Ethernet or (future) cellular telephony industry.

Acknowledgment

This research has been cofinanced by the European Union and Greek national funds through the Operational Program Competitiveness, Entrepreneurship and Innovation, under the call RESEARCH - CREATE - INNOVATE (project code: T1EDK-03032).

References

[1] G. D. Durgin, "RF thermoelectric generation for passive RFID," in *Proc. IEEE RFID*, Orlando, FL, May 2016, pp. 1–8.

[2] J. Kimionis, A. Bletsas, and J. N. Sahalos, "Design and implementation of RFID systems with software defined radio," in *Proc. IEEE European Conf. on Antennas and Propagation (EuCAP)*, Prague, Czech Republic, Mar. 2012, pp. 3464–3468.

[3] ——, "Bistatic backscatter radio for tag read-range extension," in *Proc. IEEE RFID Techn. and Applications (RFID-TA)*, Nice, France, Nov. 2012.

[4] ——, "Bistatic backscatter radio for power-limited sensor networks," in *Proc. IEEE Global Commun. Conf. (Globecom)*, Atlanta, GA, Dec. 2013, pp. 353–358.

[5] ——, "Increased range bistatic scatter radio," *IEEE Trans. Commun.*, vol. 62, no. 3, pp. 1091–1104, Mar. 2014.

[6] E. Kampianakis, J. Kimionis, K. Tountas, C. Konstantopoulos, E. Koutroulis, and A. Bletsas, "Backscatter sensor network for extended ranges and low cost with frequency modulators: Application on wireless humidity sensing," in *Proc. IEEE Sensors Conf. (Sensors)*, Baltimore, MD, USA, Nov. 2013.

[7] ——, "Wireless environmental sensor networking with analog scatter radio & timer principles," *IEEE Sensors J.*, vol. 14, no. 10, pp. 3365–3376, Oct. 2014.

[8] K. Tountas, P. N. Alevizos, A. Tzedaki, and A. Bletsas, "Bistatic architecture provides extended coverage and system reliability in scatter sensor networks," in *Proc. International EURASIP Workshop on RFID Technology (EURFID)*, Rosenheim, Germany, Oct. 2015, pp. 144–151.

[9] P. N. Alevizos, K. Tountas, and A. Bletsas, "Multistatic scatter radio sensor networks for extended coverage," *IEEE Trans. Wireless Commun.*, vol. 17, no. 7, pp. 4522–4535, Jul. 2018.

[10] J. D. Griffin and G. D. Durgin, "Gains for RF tags using multiple antennas," *IEEE Trans. Antennas Propagat.*, vol. 56, no. 2, pp. 563–570, Feb. 2008.

[11] J. F. Ensworth and M. S. Reynolds, "Every smart phone is a backscatter reader: Modulated backscatter compatibility with bluetooth 4.0 low energy (BLE) devices," in *Proc. IEEE RFID*, San Diego, CA, Apr. 2015, pp. 78–85.

[12] J. F. Ensworth and M. S. Reynolds, "BLE-Backscatter: Ultralow-Power IoT Nodes Compatible With Bluetooth 4.0 Low Energy (BLE) Smartphones and Tablets," *IEEE Transactions on Microwave Theory and Techniques*, vol. 65, no. 9, pp. 3360–3368, Sep. 2017.

[13] V. Iyer, V. Talla, B. Kellogg, S. Gollakota, and J. Smith, "Inter-technology backscatter: Towards internet connectivity for implanted devices," in *Proc. ACM SIGCOMM*, Florianopolis, Brazil, 2016, pp. 356–369.

[14] V. Talla, M. Hessar, B. Kellogg, A. Najafi, J. R. Smith, and S. Gollakota, "Lora backscatter: Enabling the vision of ubiquitous connectivity," *Proc. ACM Interact. Mob. Wearable Ubiquitous Technol.*, vol. 1, no. 3, pp. 105:1–105:24, Sep. 2017.

[15] R. Sadr *et al.*, "RFID systems using distributed exciter network," Mar. 2013, US Patent 8,395,482 B2. [Online]. Available: https://patents.google.com/patent/US8395482B2/en?oq=US8395482

[16] Z. Fu, M. J. Crisp, S. Yang, R. V. Penty, and I. H. White, "Long distance passive UHF RFID system over ethernet cable," in *Proc. IEEE RFID Techn. and Applications (RFID-TA)*, Warsaw, Poland, Sep. 2017, pp. 294–298.

[17] Y. Ma, N. Selby, and F. Adib, "Drone relays for battery-free networks," in *Proc. ACM SIGCOMM*, Los Angeles, CA, 2017.

[18] *EPC Radio-Frequency Identity Protocols, Class-1 Generation-2 UHF RFID Protocol for Communications at 860 MHZ-960 MHZ.* EPC Global, 2015, version 2.0.1.

[19] M. Buettner and D. Wetherall, "A software radio-based UHF RFID reader for PHY/MAC experimentation," in *Proc. IEEE RFID*, Apr. 2011, pp. 134–141.

[20] N. Kargas, F. Mavromatis, and A. Bletsas, "Fully-coherent reader with commodity SDR for Gen2 FM0 and computational RFID," *IEEE Wireless Commun. Lett.*, vol. 4, no. 6, pp. 617–620, Dec. 2015.

[21] M. Ouroutzoglou, G. Vougioukas, and A. Bletsas, "Multistatic noncoherent linear complexity Miller sequence detection for Gen2 RFID/IoT," *IEEE Trans. Wireless Commun.*, 2019, in preparation, to be submitted.

[22] M. Rice, *Digital Communications: A Discrete-time Approach*. Pearson/Prentice Hall, 2009.

[23] S. M. Kay, *Fundamentals of statistical signal processing. [Volume I]. , Estimation theory*. Upper Saddle River (N.J.): Prentice Hall, 1993.

[24] M. Ouroutzoglou and A. Bletsas, "Linear complexity noncoherent Miller sequence detection for batteryless RFID/IoT," in *Proc. IEEE Int. Conf. Communications*, Shanghai, P.R. China, May 2019.

[25] E. Stratigi, "Synchronization, channel estimation and detection of RFID signals with Miller coding," Diploma thesis available in: http://dias.library.tuc.gr/view/72071, School of ECE, Technical University of Crete, Chania, Greece, Feb. 2018, Supervisor A. Bletsas.